applied sciences

MDPI

Article

Concrete Composites Based on Quaternary Blended Cements with a Reduced Width of Initial Microcracks

Grzegorz Ludwik Golewski

Department of Structural Engineering, Faculty of Civil Engineering and Architecture, Lublin University of Technology, Nadbystrzycka 40 Str., 20-618 Lublin, Poland; g.golewski@pollub.pl; Tel.: +48-81-5384394; Fax: +48-81-5384390

Abstract: This article is devoted to the study of the combined effect of siliceous fly ash (FA), silica fume (SF), and nanosilica (nS) on the cement matrix morphology and size of microcracks occurring in the Interfacial Transition Zone (ITZ) between the coarse aggregate and the cement paste of concrete composites based on ordinary Portland cement (OPC). The manuscript contains analyses of width of microcracks (*Wc*) occurring in the ITZ area of concretes based on quaternary blended cements and changes in ITZ morphology in the concretes in question. Experiments were planned for four types of concrete. Three of them were composites based on quaternary blended cements (QBC), while the fourth was reference concrete (REF). Based on the observations of the matrices of individual composites, it was found that the REF concrete was characterized by the most heterogeneous structure. However, substitution of part of the cement binder with active pozzolanic additives resulted in a more compact and homogenous structure of the cement matrix in each of the QBC series concretes. Moreover, when analyzing the average *Wc* values, it should be stated that the modification of the basic structure of the cement matrix present in the REF concrete resulted in a significant reduction of the analyzed parameter in all concretes of the QBC series. For QBC-1, QBC-2, and QBC-3, the *Wc* values were 0.70 µm, 0.59 µm, and 0.79 µm, respectively, indicating a decrease of 38%, almost 48%, and 30%, respectively, compared with the working condition of concrete without additives. On the basis of the above results, it can therefore be concluded that the proposed modification of the binder composition in the analyzed materials clearly leads to homogenization of the composite structure and limitation of initial internal damages in concrete.

Keywords: concrete composite; quaternary binder concrete (QBC); morphology; microcrack width (*Wc*); siliceous fly ash (FA); silica fume (SF); nanosilica (nS); Interfacial Transition Zone (ITZ)

Citation: Golewski, G.L. Concrete Composites Based on Quaternary Blended Cements with a Reduced Width of Initial Microcracks. *Appl. Sci.* **2023**, *13*, 7338. https://doi.org/10.3390/app13127338

Academic Editors: Aniello Riccio and Angela Russo

Received: 31 May 2023
Revised: 18 June 2023
Accepted: 19 June 2023
Published: 20 June 2023

1. Introduction

Building structures made of concrete composites effectively protect against rain, moisture, noise, cold, and temperature fluctuations. In addition, the construction of buildings and structures made of concrete composites, as well as the subsequent maintenance and renovation of concrete structures, catalyze the development of world economies, thus significantly contributing to their economic progress and the increase of gross domestic products. Therefore, from an economic and social point of view, the dynamics of the development of the concrete industry is still highly desirable [1–3].

One of the most important issues in the field of concrete and reinforced concrete structures is the ability to select the components of the concrete mix, and then carry out the technological process of molding the composite structure in such a way that the concrete after the curing period in a solidified form is characterized by the lowest possible number of initial microcracks [4–6].

Having regard to the mechanical properties of cementitious materials, it is important to observe structure defects due to the fact that as stress concentrators, they constitute the cause of crack development and bring about material damage [7–9]. According to the

literature data, the area of first microcrack initiation in ordinary concretes is the Interfacial Transition Zone (ITZ) between the largest grains of coarse aggregate and the paste [10,11]. The role of this concrete phase is significant enough that according to [12–14], the mechanical parameters and the material fracture toughness is not only associated with the strength of components which form the concrete structure, but to a large extent with the parameters of all contact zones in the composite, as well as material defects occurring even before application of the load.

The width of microcracks (*W*c) in the ITZ area also has a decisive impact on the degradation processes of structures made of concrete [15,16]. All discontinuities occurring in the structure of the cement matrix and the contacts between the inclusions and the continuous phase of the composite increase its permeability, thus enabling the migration of harmful and aggressive substances deep into the material structure [17–19]. The presence of such media and their adverse impact on individual components of concrete may result in:

- Acceleration of destruction of the material from which the structure is made;
- Shortening the life of the structure;
- Reducing the level of structure operation reliability;
- Making impossible to ensure an adequate level of structure safety;
- The need for more frequent and costly repairs.

For these reasons, knowledge concerning the size of material microcracks is important from scientific, engineering, and economic points of view [20,21]. The phenomenon of cracking in concrete composites and reinforced concrete structures is described in detail in an overview study concerning this subject [22]. This article presents a detailed study of causes of crack formation in the concrete structure, and the places of their occurrence. Standard and modern methods of detecting microcracks and cracks were characterized and methods of minimizing their occurrence were outlined. It has been pointed out, among other things, that one of the methods for the design of composite structures with damage constraints is modifying the composition of the concrete mix in such a way as to obtain the smallest possible initial defects of the mature composite structure [23–25]. For this purpose, the components of the concrete mix (mainly the binders) should be selected in such a way as to achieve a synergistic effect of interaction between the individual components used [26,27]. As a result of this, it is possible to obtain a more homogenous structure of the concrete mix, resulting in a more compact structure of the hardened concrete composite [28,29].

Therefore, concretes containing binders with a modified composition have been used for many years. Such modifications consist of replacing part of ordinary Portland cement (OPC) with other mineral materials [30,31]. Substitutes for cement binder are most often additives, and in recent years also nanoadditives [32,33]. In the simplest solutions, i.e., concretes based on binary binders, OPC is replaced by only one additional component, e.g., fly ash (FA), silica fume (SF), or metakaolin (MK) [34–36]. The benefits which have been observed from such solutions include limiting the width of the initial microcracks in concretes of this type, reduction of porosity of such materials, and improving their mechanical parameters [37–39]. In most cases, however, such effects resulted from strengthening the cement matrix structure through the development of additional C-S-H and C-A-S-H phases [40–42]. Previous studies have shown, among other things, that a particularly positive effect on the microstructure of the ITZ area between coarse aggregate and paste is the modification of the composition of the cement binder with single additives and nanoadditives, such as:

- Siliceous fly ash [43];
- Silica fume [44];
- Metakaolin [45];
- Ground granulated blast furnace slag [46];
- Rice husk ash [47];
- Waste glass [48];
- Natural pozzolan [49];
- Limestone powder [50];

- Granite powder [51];
- Nanosilica [52,53];
- Carbon nanotubes [54];
- Graphene [55];
- Reactive powders [56];
- C-S-H seeds [57,58].

Benefits in reducing the microcracks in the ITZ area have been also obtained when replacing mineral aggregates with recycled aggregates [59–61] or coral aggregates [62], and using sand concretes [63]. In addition, the work [64] presents the results of tests evaluating the effect of curing time on the size of microcracks in the ITZ area in concretes with the addition of FA.

However, more advanced solutions in this field of material engineering rely on the substitution of cementitious binder with a combination of two or even three active Supplementary Cementitious Materials (SCMs) [65]. Such modifications are referred to as concretes based on ternary or quaternary binders [66,67].

As previous studies have shown, this type of concrete, in comparison with ordinary concrete, is characterized by:

- Excellent mechanical parameters, i.e., with the results exceeding the results obtained for unmodified concrete by several dozen percent;
- Fracture toughness increased by several to several dozen percent;
- A more stable crack propagation process;
- A more homogenous structure of the cement matrix.

It should also be mentioned that material modification in the form of concretes based on multi-component binders also includes pro-ecological activities. It has been proven that by reducing the consumption of OPC and the possibility of using waste materials as a substitute for the binder, such solutions cause [68–71]:

- Significant reduction of CO_2 emission;
- Reduction of electricity and heat energy;
- The possibility of waste management.

Due to the fact that material modification of concrete by a combination of several SCMs simultaneously contributes to both the improvement of properties of the composites with cement matrix and the development of sustainable construction, this article presents the results of new experiments assessing the size of microcracks in the ITZ area of such materials. The manuscript contains analyses of:

- The width of microcracks (W_c) occurring in the ITZ area of concretes based on quaternary blended cements;
- Changes in ITZ morphology in the concretes in question.

Based on the results of the experiments conducted, it will be possible to obtain information about the possibility of effective modification of concrete composites in terms of obtaining modern, innovative, and ecological materials with increased durability and increased reliability.

2. Scope of the Experimental Study

Experiments were planned for four types of concrete. Three of them were composites based on quaternary blended cements (QBC), while the fourth was a reference concrete (REF). Modification of the binder composition in QBC concretes was performed by substituting OPC with the two most commonly used mineral additives, i.e., siliceous fly ash (FA) and non-condensed silica fume (SF). In addition, as an element of modern nano-modification, synthetic nanosilica (nS) was used.

As in the previous tests of mechanical parameters, brittleness, and fracture toughness—carried out on the same materials—the following composition of the composites was assumed [72]:

- Constant SF content, equal to 10%, and nS in the amount of 5%;
- Variable FA content, the amounts of which were, respectively: 0, 5, and 15%.

Based on such assumptions, it was possible to determine the impact of basic SCMs, i.e., FA, for the structure of the contact area of the coarse aggregate with the cement matrix and size of microcracks in the ITZ area in concretes containing silica additives. The detailed compositions of individual composites are given in Section 3.2.

3. Materials and Methods

3.1. Materials

3.1.1. Aggregates

Locally available natural pit sand with 2.0 mm maximum size was used as fine aggregate, and natural gravel as coarse aggregate with 8.0 mm maximum size. Properties of both aggregates used are tabulated in Table 1, whereas their appearance is shown in Figure 1.

Table 1. Properties of fine and coarse aggregates.

Property	Unit	Aggregate Type	
		Fine Aggregate (Sand)	**Coarse Aggregate (Gravel)**
Specific density	(g/cm^3)	2.60	2.65
Bulk density	(g/cm^3)	2.20	2.25
Compressive strength	(MPa)	33	34
Modulus of elasticity	(10^2 MPa)	330	330
Sand point for mix	(%)	40.7	

(**a**) (**b**)

Figure 1. Appearance of aggregates used: (**a**) sand, (**b**) gravel.

3.1.2. Binders

Concrete mixtures were made using the following binders:

- OPC CEM I 32.5 R;
- Siliceous FA;
- Non-condensed SF;
- nS Konasil K-200.

The chemical compositions and physical properties of the binders used are shown in Tables 2 and 3, respectively. In addition, the appearance of all binders is presented in Figure 2.

Table 2. Chemical composition of the binders used (% mass).

Material\Constituent	SiO_2	Al_2O_3	CaO	MgO	SO_3	Fe_2O_3	K_2O	P_2O_5	TiO_2	Ag_2O
OPC	15.00	2.78	71.06	1.38	4.56	2.72	1.21	-	-	-
FA	55.27	26.72	2.35	0.81	0.47	6.66	3.01	1.92	1.89	0.10
SF	91.90	0.71	0.31	1.14	0.45	2.54	1.53	0.63	0.01	0.07
nS	>99.8	-	-	-	-	-	-	-	-	-

Table 3. Physical characteristics of binders used.

Physical Parameter	Kind of Binder			
	OPC	FA	SF	nS
Specific gravity (g/cm^3)	3.11	2.14	2.21	1.10
Blaine's fineness (m^2/g)	0.33	0.36	1.40	200
Average particle diameter (μm)	40	30	11	0.012

Figure 2. Appearance of binders used: (**a**) OPC, (**b**) FA, (**c**) SF, (**d**) nS.

3.1.3. Water

In order to prepare concrete mixtures, tap water (W) was used which met the requirements of the standard provision EN 1008:2002 [73].

3.1.4. Admixture

In order to improve the flowability of the concrete mixtures, a superplasticizer (SP), STACHEMENT 2750, based on polycarboxylates, was used.

3.2. Mixture Design and Manufacturing Process

The concrete mixture proportions are summarized in Table 4. All mixtures had the same water–binder ratio w/b = 0.4.

Table 4. Mix proportions (kg/m^3).

Mix	OPC	%OPC	FA	%FA	SF	%SF	nS	%nS	Water	SP	Sand	Gravel
REF	352	100	0	0	0	0	0	0	141	0	676	1205
QBC-1	299.2	85	0	0	35.2	10	17.6	5	141	6	676	1205
QBC-2	281.6	80	17.6	5	35.2	10	17.6	5	141	6	676	1205
QBC-3	246.4	70	52.8	15	35.2	10	17.6	5	141	6	676	1205

The samples were made in a special room located at the laboratory of the Faculty of Civil Engineering and Architecture, Lublin University of Technology (Lublin, Poland). The components for making concrete mixtures listed in Table 4 were weighed on two scales with different ranges, i.e.,:

- FaWag TP150/1 1D34ABM (range: 1–150 kg);
- RadWag WLC 30/C1/R (range: 0–30 kg).

The process of making concrete mixes was carried out in the DZB-300 counter-rotating mixer with a capacity of 150 L and power of 1.1 kW. The time needed to prepare the concrete mix for one batch of samples was approx. 9–10 min. The process of mixing its components included the following basic steps:

- Mix gravel and sand in a drum mixer for 120 s;
- Add the binding materials, i.e., OPC, FA, and SF, and mix for 180 s;
- Add the mixture of water, SP, and nS, and mix for 120 s;
- Add the remaining water and mix to obtain a homogenous mixture for 120–180 s.

From the concrete mix prepared according to the above procedure, concrete specimens were then formed in the shape of cubes with a side length of 150 mm. The specimens were made in accordance with the EN 12390-2:2019 standard [74]. For this purpose, the concrete mix was laid in two layers. Each layer was compacted for a period of 30 s on the vibration table Controls C-161/LC at a frequency of 50 Hz (3000 vibrations/min). After compaction, the upper surface of the specimens was rubbed. Then, specimens were placed on the laboratory floor and covered with polyethylene foil. Successive care of the covered specimens was carried out by additional wetting every few hours. A view of the specimens during the early care process is shown in Figure 3. The black color of the cubes visible in Figure 3 is the result of the use of SF (Figure 2c) in the production of QBC series concretes.

Figure 3. View of specimens during the care process.

The specimens were demolded 24 h after their preparation and then transferred to a tub filled with water, with automatic stabilization of temperature conditions. In this way,

they were kept in water for 14 days. After this period, the specimens were taken out of the water and placed on wooden pallets, where they remained for another 14 days, until macroscopic examinations were carried out. During this period, specimens were cured in laboratory conditions at t = 20 ± 2 °C and RH = 40%.

3.3. SEM Samples and SEM Studies

In order to trace the combined impact of FA, SF, and nS particles on changes in the ITZ structure and the size of microcracks at the contact of the coarse aggregate with the cement matrix in concretes based on quaternary blended cements, microstructural analysis was carried out. Experiments were performed after 28 days of curing of composites. The impact of the applied SCMS on the analyzed parameters was assessed using a scanning electron microscope (SEM). Samples for SEM analysis were taken from cubes damaged after strength tests, described in [66,72]. A view of several samples prepared for SEM tests is shown in Figure 4. Moreover, Table 5 contains relevant data related to the sample preparation process and the main assumptions used in the SEM tests.

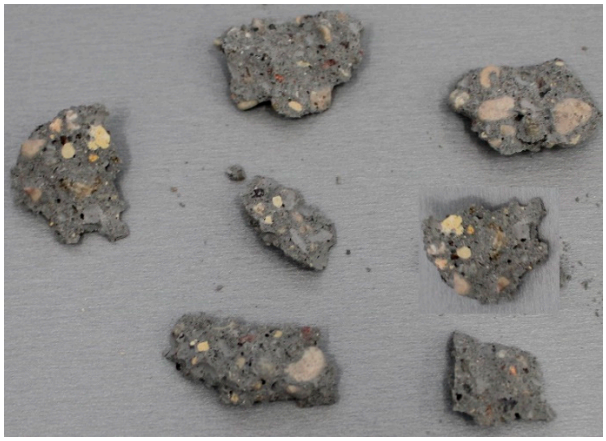

Figure 4. View of samples prepared for SEM tests.

Table 5. The main data regarding microscopic examinations.

Parameter Type	Parameter Characteristics
Microscope used in the study	Quanta FEG 250
The shape of the samples	Rectangular cube
Sample dimensions	10 × 10 × 3 mm
Samples for testing	Taken as raw—the samples before the test were not polished or prepared in any other way
The course of the experiments	The tests were performed in both low and high vacuum
Sample preparations	• In the case of tests in a high vacuum, the samples were dried for one hour at the temperature of 70 °C and then sprayed with carbon or alloy of gold and palladium in a high-vacuum sputter coater, Q 150 E; the thickness of the coated layer was about 50 nm, • In the case of the samples tested in a low vacuum, they did not require drying and spraying prior to testing
Number of samples	Six samples for each series of concrete

Table 5. *Cont.*

Parameter Type	Parameter Characteristics
Number of photos per sample	Thirty photos were taken for each sample, from which the representative photos were selected
The observed area of each concrete batch	About 3000 mm^2
Places included in the microscopic assessment	• Structure of the cement matrix • ITZ area
Magnifications used	• Basic: 8000 and 16,000 times • Additional: from 30,000 to 240,000 times

4. Results and Discussion

Figures 5–8 show exemplary representative images of the microstructure of individual tested composites. In accordance with the assumptions described in the first section of the manuscript, the analyses focused on both the assessment of morphological changes in the cement matrix and the measurements of the size of microcracks in the ITZ area of each concrete. Therefore, each of the drawings shows two characteristic areas at two basic magnifications, i.e., 8000× and 16,000×. In addition, in the case of concretes of the QBC series, the places of contact between the coarse aggregate and the paste were imaged at additional, very large magnifications. In this case, the following magnifications of the ITZ area were applied, respectively: 30,000×, 60,000×, and even 240,000×. In addition, in order to better highlight the changes in the structure of the analyzed concretes, all significant details observed were also marked on the selected representative photos. These included:

- Main phases occurring in the cement matrix,
- Areas of microcracks in the ITZ area, with the indication of their exact dimensions in three places,
- Areas of occurrence of FA grains in the paste structure,
- Voids after separation of FA grains from the cement matrix.

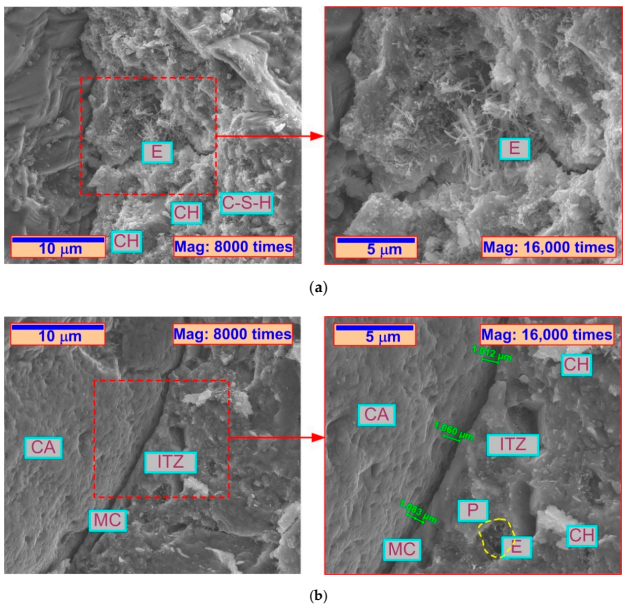

Figure 5. SEM microimages of analyzed REF concrete: (**a**) matrix area, (**b**) ITZ area; E—Ettringite, CH—Calcium Hydroxide, C-S-H—Calcium Silicate Hydrate, CA—Coarse aggregate, MC—Microcrack, P—Pore, ITZ–Interfacial Transition Zone.

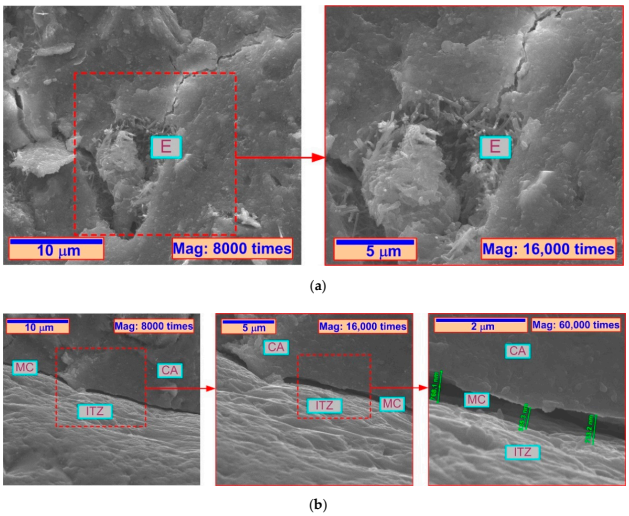

Figure 6. SEM microimages of analyzed QBC-1 concrete: (**a**) matrix area, (**b**) ITZ area; E, MC, CA, ITZ—as in Figure 6.

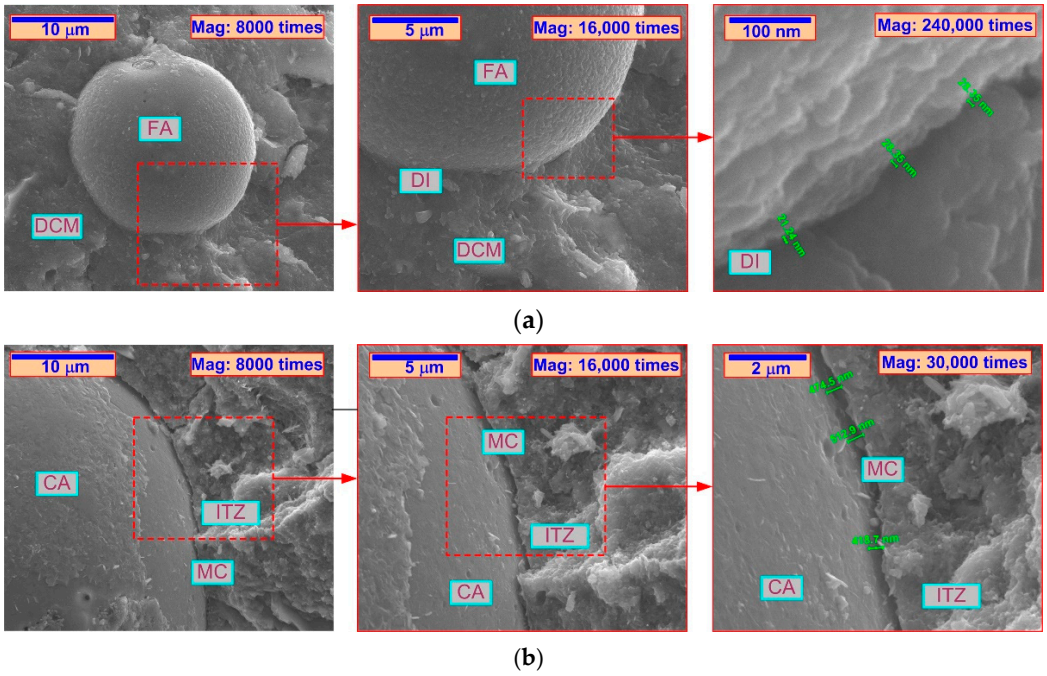

Figure 7. SEM microimages of analyzed QBC-2 concrete: (**a**) matrix area, (**b**) ITZ area; MC, CA, ITZ—as in Figure 6, FA—fly ash, DCM—dense cement matrix, DI—dense interface.

Table 6 describes the characteristic details visible in the cement matrix of all composites. In this table, attempts were made to briefly list the three most characteristic features that were most often visible in individual series of composites. In addition, the observed average microcracks width (*W*c) with error bars in the ITZ area of all composites are given in Figure 9.

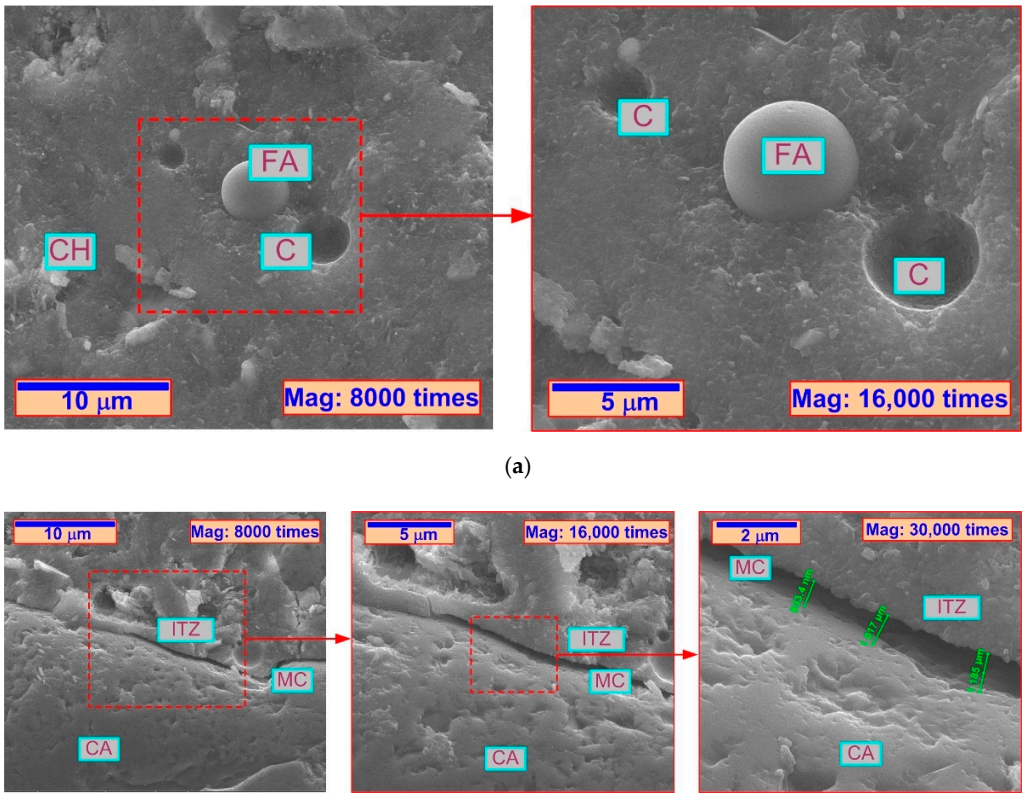

Figure 8. SEM microimages of analyzed QBC-3 concrete: (**a**) matrix area, (**b**) ITZ area; CH, MC, CA, FA, ITZ—as in Figures 6 and 8, C—Cavity after separation of FA particles.

Table 6. Morphology of the cement matrix of analyzed concretes.

Mix	Morphological Characteristics of Cement Matrix
REF	• Clear heterogeneity; • Visible large number of phases during reaction, mainly in the form of ettringite and portlandite, and the C-S-H phase to a lesser extent; • Visible microcracks located in the structure of the matrix;
QBC-1	• Slightly compact structure; • Visible porous areas filled with the ettringite (E) phase; • Visible small microcracks in the matrix;
QBC-2	• Dense and homogenous structure (a lot of DCM areas were visible); • The cement matrix looked the most homogenized; • FA grains were well embedded in the paste;
QBC-3	• Almost dense and homogenous structure; • The ettringite and portlandite phases during reaction were visible; • Cavities in the matrix after the separation of FA grains were visible.

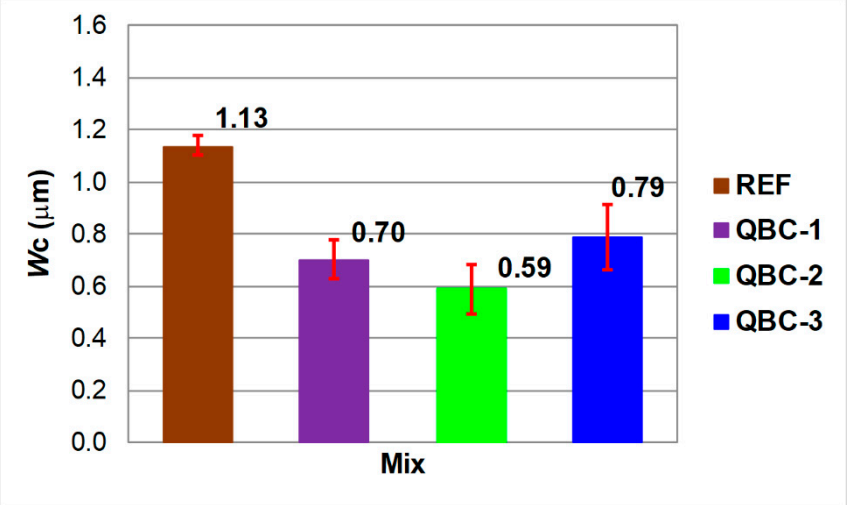

Figure 9. Results of microcrack width of analyzed concretes.

Based on the observations of the matrices of individual composites presented in Table 5, it was found that the reference concrete was characterized by the most heterogeneous structure. Most of the phases present in this material were still in the process of reacting. Microcracks in the cement matrix were also observed (Figure 5a).

Substitution of part of the cement binder with active pozzolanic additives resulted in a more compact and homogenous structure of the cement matrix in each of the QBC series concretes. However, the addition of only SF and nS in the concrete of the QBC-1 series caused only a slight change in the morphology of the matrix. In its structure, porous places were still visible, with agglomerates of concrete phases occurring therein during the reaction (Figure 6a). Nevertheless, the surface of the fracture in this concrete was already clearly more compact than in the REF concrete.

In the concrete of the QBC-2 series, which contained both silica and FA additives in 5% quantities, the structure of the matrix was clearly compact, while FA grains visible in the paste were well integrated with the paste. Their contact with the surface of the matrix was compact, with almost imperceptible microdamages at the level of 20 nm (Figure 7a). In this composite, it was possible to clearly observe the synergy effect occurring between the three SCMs used.

Increasing the amount of FA in the binder composition resulted in the effect of weakening the quality of the matrix structure. In this composite, i.e., QBC-3 series, unreacted FA grains had weak bonds with the paste surface. The places after their separation were also partly visible (Figure 8a). The structure of the cement matrix was also less compact than in the case of concrete with a lower FA content, i.e., QBC-2 (Figure 7a).

Therefore, the results of microstructural tests of concrete containing FA confirm the earlier results given, among others, in [75]. On this basis, it can be concluded that the beneficial effect of FA additive in strengthening the structure of the cement matrix becomes evident in the case of using this useful waste only to a certain level. In the case of concretes modified by FA only, this is in the range not exceeding 20% [76–78]. However, in the case of composites based on ternary or quaternary blended cements, the level of OPC substitution by FA should be much lower, preferably at the level of several percent [79,80].

After carrying out the microstructural assessment of individual composites, an analysis of the size of microcracks occurring in the ITZ area of the concrete in question was also performed. Based on the observations of the paste morphology in each of the materials, attempts were made to link these data with the results of *Wc* measurements.

When analyzing the average *Wc* values, it should be stated that the modification of the basic structure of the cement matrix present in the REF concrete resulted in a significant reduction of the analyzed parameter in all concretes of the QBC series (Figure 9). This is

due to the fact that for the QBC-1, QBC-2, and QBC-3, the microcrack width of concrete composites was 0.70 µm, 0.59 µm, and 0.79 µm, respectively, indicating a decrease of 38%, almost 48%, and 30%, respectively, compared with the result obtained for concrete without additives.

Observed relationships are clearly visible when comparing the relative changes of *Wc* in each of the concretes containing SCMs, compared to the result obtained for the reference concrete. This is shown in Figure 10.

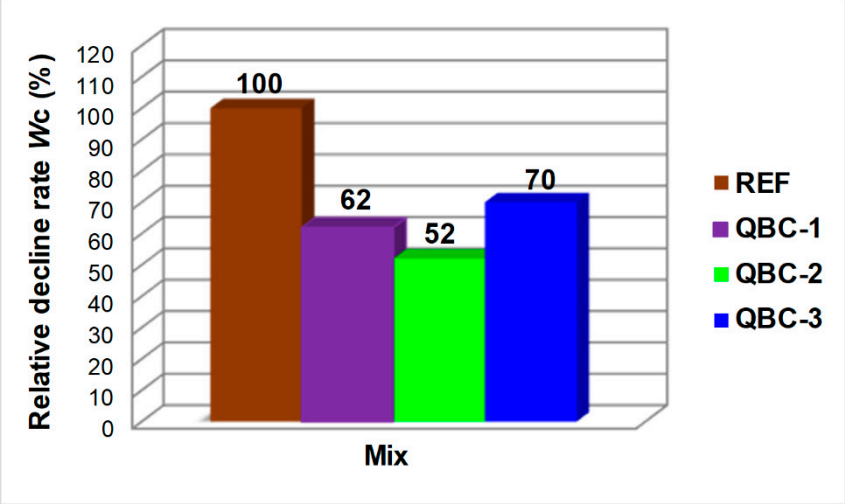

Figure 10. Relative decline rate of microcrack width of analyzed concretes.

In addition, it should be stated that with a more advanced modification of the basic composition of the binder, the obtained *Wc* results were less convergent, i.e., the size of the error bars in the average values of the analyzed parameter for QBC series concretes increased significantly. This was most clearly visible in concretes containing all three SCMs (Figure 9). A larger dispersion of test results was also observed earlier in the study of mechanical parameters, and the parameters of the fracture mechanics of the same composites [81,82]. This phenomenon is probably caused by the heterogeneous reaction of FA grains or their partial separation from the matrix structure in the QBC-3 series concrete. This, in turn, has an impact on increased dispersions in the results obtained in concrete with these additives.

On the basis of the above results, it can therefore be concluded that the proposed modification of the binder composition in the analyzed materials clearly leads to:

- Homogenization of the composite structure;
- Limitation of initial internal damages in concrete.

The synergy between the additives and the nanoadditive used, which appeared during the formation of the cement matrix structure, made it more homogenous and less porous. In the case of QBC-2 and partly QBC-3 series concrete, it was completely homogenized. This, in the case of concrete modified with three active pozzolanic materials, led to the size of microcracks in the ITZ area of coarse aggregate with the paste being significantly reduced. The average values of *Wc* decreased compared to the values obtained for the reference concrete (Figure 10):

- By almost 40% in the case of QBC-1 series concrete;
- By almost half in the concrete of the QBC-2 series;
- By 30% in concrete of the QBC-3 series.

Thanks to such favorable research results, it is possible to obtain composites that are less susceptible to damage and thus more durable, and do not require frequent repairs. This, in turn, reduces the global operating costs of buildings made of this type of material.

5. Conclusions

From the above data, it can be stated that the introduction of pozzolanic additives in the form of FA and SF, in combination with a very reactive nanoadditive, which is nS, accelerate the hardening of concrete composites after 28 days of their curing. At the same time, the most noticeable effect observed was of reducing microcracks in the ITZ area in concretes based on quaternary blended cements including 10%SF + 5%FA + 5%nS. Therefore, taking into account the results of the research carried out, it can be concluded that:

1. The addition of three pozzolanic materials, i.e., FA, SF, and nS in combination, modifies the microstructure of the cement matrix and ITZ area.
2. Reference concrete is characterized by greater microcrack width in the ITZ area in comparison to the concretes based on quaternary blended cements.
3. The smallest microcracks occur in concrete with 10%SF+5%FA+5%nS. This shows that the composite of the QBC-2 series is characterized by high durability.
4. In the case of concretes modified with three active pozzolanic materials, the sizes of microcracks in the ITZ between the coarse aggregate and the paste are clearly reduced.

Funding: The research leading to these results received funding from the MINIATURA 2 Grant, No. 2018/02/X/ST8/02726: funded by National Science Center of Poland.

Institutional Review Board Statement: Not applicable.

Informed Consent Statement: Not applicable.

Data Availability Statement: No new data were created or analyzed in this study. Data sharing is not applicable to this article.

Conflicts of Interest: The author declares no conflict of interest.

References

1. Liu, F.; Zou, Y.; Wang, B.; Yuan, X. The Effect of Stray Current on Calcium Leaching of Cement-Based Materials. *Materials* **2022**, *15*, 2279. [CrossRef] [PubMed]
2. Wardach, M.; Krentowski, J.R.; Mackiewicz, M. Evaluation of precast beam deflections resulting in cracks in curtain walls. *Eng. Fail. Anal.* **2022**, *140*, 106568. [CrossRef]
3. Golewski, G.L. The specificity of shaping and execution of monolithic pocket foundations (PF) in hall buildings. *Buildings* **2022**, *12*, 192. [CrossRef]
4. Miraldo, S.; Lopes, S.; Pcheco-Torgal, F.; Lopes, A. Advantages and shortcomings of the utilization of recycled wastes as aggregates in structural concretes. *Constr. Build. Mater.* **2021**, *298*, 123729. [CrossRef]
5. Kovacik, J.; Marsavina, L.; Linul, E. Poisson's ratio of closed-cell aluminum foams. *Materials* **2018**, *11*, 1904. [CrossRef]
6. Zhang, P.; Wang, C.; Gao, Z.; Wang, F. A Review on Fracture Properties of Steel Fiber Reinforced Concrete. *J. Build. Eng.* **2023**, *67*, 105975. [CrossRef]
7. Abdulrahman, H.; Muhamad, R.; Visitin, P.; Shukri, A.A. Mechanical properties and bond stress-slip behaviour of fly ash geopolymer concrete. *Constr. Build. Mater.* **2022**, *327*, 126909. [CrossRef]
8. Craciun, E.M. Energy criteria for crack propagation in prestresses elastic composites. *Sol. Mech. Appl.* **2008**, *154*, 193–237.
9. Golewski, G.L.; Szostak, B. Strength and Microstructure of Composites with Cement Matrixes Modified by Fly Ash and Active Seeds of C-S-H Phase. *Struct. Eng. Mech.* **2022**, *82*, 543–556.
10. Kong, Y.; Wang, P.; Liu, S.; Zhao, G.; Peng, Y. SEM Analysis of the Interfacial Transition Zone between Cement-Glass Powder Paste and Aggregate of Mortar under Microwave Curing. *Materials* **2016**, *9*, 733. [CrossRef]
11. Shahsavar, S.; Fakoor, M.; Berto, F. Mixed Mode I/II Fracture Criterion to Anticipate Cracked Composite Materials Based on Reinforced Kinked Crack Along Maximum Shear Stress Path. *Stell Compos. Struct.* **2021**, *39*, 765–779.
12. Golewski, G.; Sadowski, T. Fracture Toughness at Shear (Mode II) of Concretes Made of Natural and Broken Aggregates. *Brittle Matrix Compos.* **2006**, *8*, 537–546.
13. Hashemmoniri, S.; Fatemi, A. Optimization of Lightweight Foamed Concrete Using Fly Ash Based on Mechanical Properties. *Inn. Infrastruct. Sol.* **2023**, *8*, 59. [CrossRef]
14. Reis, J.M.L.; Chianelli-Junior, R.; Cardoso, J.L.; Marinho, F.J.V. Effect of Recycled PET in the Fracture Mechanics of Polymer Mortar. *Constr. Build. Mater.* **2011**, *25*, 2799–2804. [CrossRef]
15. Golewski, G.L.; Sadowski, T. Macroscopic Evaluation of Fracture Processes in Fly Ash Concrete. *Sol. State. Phenom.* **2016**, *254*, 188–193. [CrossRef]
16. Li, X.; Zhang, Q. Influence Behavior of Phosphorus Slag and Fly Ash on the Interface Transition Zone in Concrete Prepared by Cement-Red Mud. *J. Build. Eng.* **2021**, *49*, 104017. [CrossRef]

17. Rong, G.; He, T.; Zhang, G.; Li, Y.; Wang, Y.; Xie, W. A Review on Chloride Transport Model and Research Method in Concrete. *Mater. Res. Express* **2023**, *10*, 042002. [CrossRef]
18. Golewski, G.L. Changes in the Fracture Toughness under Mode II Loading of Low Calcium Fly Ash (LCFA) Concrete Depending on Ages. *Materials* **2020**, *13*, 5241. [CrossRef]
19. Fu, Q.; Zhang, Z.; Wang, Z.; He, J.; Niu, D. Erosion Behavior of Ions in Lining Concrete Incorporating Fly Ash and Silica Fume under the Combined Action of Load and Flowing Groundwater Containing Composite Salt. *Case Stud. Constr. Mater.* **2022**, *17*, e01659. [CrossRef]
20. Gil, D.M.; Golewski, G.L. Potential of Siliceous Fly Ash and Silica Fume as a Substitute of Binder in Cementitious Concrete. *E3S Web Conf.* **2018**, *49*, 00030. [CrossRef]
21. Riccio, A.; Castaldo, R.; Palumbo, C.; Russo, A. Delamination Effect on the Buckling Behaviour of Carbon–Epoxy Composite Typical Aeronautical Panels. *Appl. Sci.* **2023**, *13*, 4358. [CrossRef]
22. Golewski, G.L. The Phenomenon of Cracking in Cement Concretes and Reinforced Concrete Structures: The Mechanism of Cracks Formation, Causes of Their Initiation, Types and Places of Occurrence, and Methods of Detection—A Review. *Buildings* **2023**, *13*, 765. [CrossRef]
23. Golewski, G.L. Determination of Fracture Toughness in Concretes Containing Siliceous Fly Ash during Mode III Loading. *Struct. Eng. Mech.* **2017**, *62*, 1–9. [CrossRef]
24. Chen, S.; Wang, H.; Guan, J.; Yao, X.; Li, L. Determination Method and Prediction Model of Fracture and Strength of Recycled Aggregate Concrete at Different Curing Ages. *Constr. Build. Mater.* **2022**, *343*, 128070. [CrossRef]
25. Guan, J.; Yin, Y.; Li, Y.; Yao, X.; Li, L. A Design Method for Determining Fracture Toughness and Tensile Strength Pertinent to Concrete Sieving Curve. *Eng. Fract. Mech.* **2022**, *271*, 108596. [CrossRef]
26. Wei, J.; Liu, J.; Khayat, K.H.; Long, W.-J. Synergistic Effect of HEDP.4Na and Different Induced Pouring Angles on Mechanical Properties of Fiber-Reinforced Alkali-Activated Slag Composites. *Fibers* **2023**, *11*, 23. [CrossRef]
27. Golewski, G.L. Combined Effect of Coal Fly Ash (CFA) and Nanosilica (Ns) on the Strength Parameters and Microstructural Properties of Eco-Friendly Concrete. *Energies* **2023**, *16*, 452. [CrossRef]
28. Suchorab, Z.; Franus, M.; Barnat-Hunek, D. Properties of Fibrous Concrete Made with Plastic Fibers from E-Waste. *Materials* **2020**, *13*, 2414. [CrossRef]
29. Golewski, G.L.; Sadowski, T. A Study on Mode III Fracture Toughness in Young and Mature Concrete with Fly Ash Additive. *Solid State Phenom.* **2016**, *254*, 120–125. [CrossRef]
30. Ahmad, J.; Zaid, O.; Shahzaib, M.; Usman Abdullah, M.; Ullah, A.; Ullah, R. Mechanical properties of sustainable concrete modified by adding marble slurry cement substitution. *AIMS Mater. Sci.* **2021**, *8*, 343–358. [CrossRef]
31. Pacheco-Torgal, F. High Tech Startup Creation for Energy Efficient Built Environment. *Renew. Sustain. Energy Rev.* **2017**, *71*, 618–629. [CrossRef]
32. Alex, A.G.; Kemal, Z.; Gebrehiwet, T.; Getahun, S. Effect of a: Phase Nano Al_2O_3 and Rice Husk Ash in Cement Mortar. *Adv. Civ. Eng.* **2022**, *2022*, 4335736. [CrossRef]
33. Wang, L.; Zhang, P.; Golewski, G.L.; Guan, J. Editorial: Fabrication and Properties of Concrete Containing Industrial Waste. *Front. Mater.* **2023**, *10*, 1169715. [CrossRef]
34. Szcześniak, A.; Zychowicz, J.; Stolarski, A. Influence of Fly Ash Additive on the Properties of Concrete with Slag Cement. *Materials* **2020**, *13*, 3265. [CrossRef]
35. Xie, T.; Yang, G.; Zhao, X.; Xu, J.; Fang, C. A unified model for predicting the compressive strength of recycled aggregate concrete containing supplementary cementitious materials. *J. Clean. Prod.* **2020**, *251*, 119752. [CrossRef]
36. Golewski, G.L. Studies of natural radioactivity of concrete with siliceous fly ash addition. *Cem. Wapno Beton* **2015**, *2*, 106–114.
37. Adam, M.G.O.; Koteng, D.O.; Ng'ang'a Thuo, J.; Matallah, M. Effects of Acid Attack and Cassava Flour Dosage on the Interfacial Transition Zone Thickness, Durability and Mechanical Characteristics of High-Strength (HS) Concrete. *Res. Eng.* **2023**, *17*, 101001.
38. Aghajanian, A.; Cimentada, A.; Fayyaz, M.; Brand, A.S.; Thomasa, C. ITZ Microanalysis of Cement-Based Building Materials with Incorporation of Siderurgical Aggregates. *J. Build. Eng.* **2023**, *67*, 106008. [CrossRef]
39. Golewski, G.L. Mechanical Properties and Brittleness of Concrete Made by Combined Fly Ash, Silica Fume and Nanosilica with ordinary Portland cement. *AIMS Mater. Sci.* **2023**, *10*, 390–404. [CrossRef]
40. Zeyad, A.M.; Tayeh, B.A.; Yusuf, M.O. Strength and transport characteristics of volcanic pumice powder based high strength concrete. *Constr. Build. Mater.* **2019**, *216*, 314–324. [CrossRef]
41. Gao, Y.; Jing, H.; Yu, Z.; Li, L.; Wu, J.; Chen, W. Particle size distribution of aggregate effects on the reinforcing roles of carbon nanotubes in enhancing concrete ITZ. *Constr. Build. Mater.* **2022**, *327*, 126964. [CrossRef]
42. Fattouh, M.S.; Elsayed, E.K. Influence of Utilizing Glass Powder with Silica Fume on Mechanical Properties and Microstructure of Concrete. *Delta Univ. Sci. J.* **2023**, *6*, 111–122. [CrossRef]
43. Golewski, G.L. The Role of Pozzolanic Aactivity of Siliceous Fly Ash in the Formation of the Structure of Sustainable Cementitious Composites. *Sustain. Chem.* **2022**, *3*, 520–534. [CrossRef]
44. Huang, H.-S.; Zhang, H.-Y.; Lv, Y.-M.; Chen, Y.-J. Performance and Optimization Design of High-Strength Geopolymer Cold-bonded Lightweight Aggregate: Effect of Silica Fume. *Case Stud. Constr. Mater.* **2023**, *18*, e02047. [CrossRef]
45. Lopes, A.; Lopes, S.; Fernandes, M. Time Evolution of the Modulus of Elasticity of Metakaolin-Based Geopolymer. *Appl. Sci.* **2023**, *13*, 2179. [CrossRef]

46. Neves, A.; Almeida, J.; Cruz, F.; Miranda, T.; Cunha, V.M.C.F.; Rodrigues, M.; Costa, J.; Pereira, E.B. Design Procedures for Sustainable Structural Concretes Using Wastes and Industrial By-Products. *Appl. Sci.* **2023**, *13*, 2087. [CrossRef]
47. Zhang, W.; Liu, H.; Liu, C. Impact of Rice Husk Ash on the Mechanical Characteristics and Freeze–Thaw Resistance of Recycled Aggregate Concrete. *Appl. Sci.* **2022**, *12*, 12238. [CrossRef]
48. Kuri, J.C.; Hosan, A.; Shaikh, F.U.A.; Biswas, W.K. The Effect of Recycled Waste Glass as a Coarse Aggregate on the Properties of Portland Cement Concrete and Geopolymer Concrete. *Buildings* **2023**, *13*, 586. [CrossRef]
49. Golewski, G.L. Effect of Fly Ash Addition on the Fracture Toughness of Plain Concrete at Third Model of Fracture. *J. Civ. Eng. Manag.* **2017**, *23*, 613–620. [CrossRef]
50. Alyousef, R.; Abbass, W.; Aslam, F.; Ali Gillani, S.A. Characterization of High-Performance Concrete using Limestone Powder and Supplementary Fillers in Binary and Ternary Blends under Different Curing Regimes. *Case Stud. Constr. Mater.* **2023**, *18*, e02058. [CrossRef]
51. Gil, D.M.; Golewski, G.L. Effect of Silica Fume and Siliceous Fly Ash Addition on the Fracture Toughness of Plain Concrete in Mode I. *IOP Conf. Ser. Mater. Sci. Eng.* **2018**, *416*, 012065. [CrossRef]
52. Golewski, G.L. Study of Strength and Microstructure of a New Sustainable Concrete Incorporating Pozzolanic Materials. *Struct. Eng. Mech.* **2023**, *86*, 431–441.
53. Wang, J.; Lu, X.; Ma, B.; Tan, H. Cement-Based Materials Modified by Colloidal Nano-Silica: Impermeability Characteristic and Microstructure. *Nanomaterials* **2022**, *12*, 3176. [CrossRef] [PubMed]
54. Zhang, P.; Su, J.; Guo, J.; Hu, S. Influence of Carbon Nanotube on Properties of Concrete: A Review. *Constr. Build. Mater.* **2023**, *369*, 130388. [CrossRef]
55. Zhang, P.; Wang, M.; Han, X.; Zheng, Y. A Review on Properties of Cement-Based Composites Doped with Graphene. *J. Build. Eng.* **2023**, *70*, 106367. [CrossRef]
56. Kathirvel, P.; Murali, G. Effect of using Available GGBFS, Silica Fume, Quartz Powder and Steel Fibres on the Fracture Behavior of Sustainable Reactive Powder Concrete. *Constr. Build. Mater.* **2023**, *375*, 130997. [CrossRef]
57. Yuan, B.; Wang, H.; Jin, D.; Chen, W. C-S-H Seeds Accelerate Early Age Hydration of Carbonate-Activated Slag and the Underlying Mechanism. *Materials* **2023**, *16*, 1394. [CrossRef]
58. Cuesta, A.; Morales-Cantero, A.; De la Torre, A.G.; Aranda, M.A.G. Recent Advances in C-S-H Nucleation Seeding for Improving Cement Performances. *Materials* **2023**, *16*, 1462. [CrossRef]
59. Golewski, G.L. Generalized Fracture Toughness and Compressive Strength of Sustainable Concrete Including Low Calcium Fly Ash. *Materials* **2017**, *10*, 1393. [CrossRef]
60. Sun, D.; Huang, W.; Liu, K.; Ma, R.; Wang, A.; Guan, Y.; Shen, S. Effect of the Moisture Content of Recycled Aggregate on the Mechanical Performance and Durability of Concrete. *Materials* **2022**, *15*, 6299. [CrossRef]
61. Tang, W.; Khavarian, M.; Yousefi, A.; Landenberger, B.; Cui, H. Influence of Mechanical Screened Recycled Coarse Aggregates on Properties of Self-Compacting Concrete. *Materials* **2023**, *16*, 1483. [CrossRef] [PubMed]
62. Zhang, B.; Zhu, H.; Lu, F. Fracture Properties of Slag-Based Alkali-Activated Seawater Coral Aggregate. *Theor. Appl. Fract. Mech.* **2019**, *115*, 103071. [CrossRef]
63. Sun, Z.; Xiong, J.; Cao, S.; Zhu, J.; Jia, X.; Hu, Z.; Liu, K. Effect of Different Fine Aggregate Characteristics on Fracture Toughness and Microstructure of Sand Concrete. *Materials* **2023**, *16*, 2080. [CrossRef] [PubMed]
64. Golewski, G.L. An assessment of microcracks in the Interfacial Transition Zone of durable concrete composites with fly ash additives. *Compos. Struct.* **2018**, *200*, 515–520. [CrossRef]
65. He, W.; Li, B.; Meng, X.; Shen, Q. Compound Effects of Sodium Chloride and Gypsum on the Compressive Strength and Sulfate Resistance of Slag-Based Geopolymer Concrete. *Buildings* **2023**, *13*, 675. [CrossRef]
66. Golewski, G.L. Fracture Performance of Cementitious Composites Based on Quaternary Blended Cements. *Materials* **2022**, *15*, 6023. [CrossRef]
67. Dipta, O.B.; Sobhan, S.F.; Shuvo, A.K. Assessment of the Combined Effect of Silica Fume, Fly Ash, and Steel Slag on the Mechanical Behavior of Concrete. *J. Civ. Eng. Constr.* **2023**, *12*, 78–85. [CrossRef]
68. Ramesh, G. Green concrete: Environment friendly solution. *Ind. J. Des. Eng.* **2021**, *1*, 13–20.
69. Golewski, G.L.; Sadowski, T. Experimental Investigation and Numerical Modelling Fracture Processes in Fly Ash Concrete at Early Age. *Solid State Phenom.* **2012**, *188*, 158–163. [CrossRef]
70. Piyarat, N.; Wangrakdiskul, U.; Maingam, P. Investigations of the influence of various industrial waste materials containing rice husk ash, waste glass, and sediment soil for eco-friendly production of non-fired tiles. *AIMS Mater. Sci.* **2021**, *8*, 469–485. [CrossRef]
71. Szostak, B.; Golewski, G.L. Effect of nano admixture of CSH on selected strength parameters of concrete including fly ash. *IOP Conf. Ser. Mater. Sci. Eng.* **2018**, *416*, 012105. [CrossRef]
72. Golewski, G.L. An Extensive Investigations on Fracture Parameters of Concretes Based on Quaternary Binders (QBC) by Means of the DIC Technique. *Constr. Build. Mater.* **2022**, *351*, 128823. [CrossRef]
73. *EN 1008:2002*; Mixing Water for Concrete—Specification for Sampling, Testing and Assessing the Suitability of Water, Including Water Recovered from Processes in the Concrete Industry, as Mixing Water for Concrete. British Standards Institution (BSI): London, UK, 2002.

74. *EN 12390-2:2019*; Testing Hardened Concrete–Part 2: Making and Curing Specimens for Strength Tests. British Standards Institution (BSI): London, UK, 2019.
75. Zhang, M.H. Microstructure, Crack Propagation, and Mechanical Properties of Cement Pastes Containing High Volumes of Fly Ashes. *Cem. Concr. Res.* **1995**, *25*, 1165–1178. [CrossRef]
76. Ho, D.W.S.; Lewis, R.K. Effectiveness of Fly Ash for Strength and Durability of Concrete. *Cem. Concr. Res.* **1985**, *15*, 793–800. [CrossRef]
77. Fraay, A.L.A.; Bijen, J.M.; de Haan, Y.M. The Reaction of Fly Ash in Concrete. A Critical Examination. *Cem. Concr. Res.* **1989**, *19*, 235–246. [CrossRef]
78. Lam, L.; Wong, Y.L.; Poon, C.S. Effect of Fly Ash and Silica Fume on Compressive and Fracture Behaviors of Concrete. *Cem. Concr. Res.* **1998**, *28*, 271–283. [CrossRef]
79. Patel, N.; Dave, R.; Modi, S.; Joshi, C.; Vora, S.; Solanki, M. Effect of Binary and Quaternary Blends on Compressive Strength. *Int. J. Civ. Eng. Technol.* **2016**, *7*, 242–246.
80. El-Chabib, H.; Ibrahim, A. The Performance of High-strength Flowable Concrete Made with Binary, Ternary, or Quaternary Binder in Hot Climate. *Constr. Build. Mater.* **2013**, *47*, 245–253. [CrossRef]
81. Golewski, G.L. Comparative Measurements of Fracture Toughness Combined with Visual Analysis of Cracks Propagation Using the DIC Technique of Concretes Based on Cement Matrix with a Highly Diversified Composition. *Theor. Appl. Fract. Mech.* **2022**, *121*, 103553. [CrossRef]
82. Golewski, G.L. An Analysis of Fracture Toughness in Concrete with Fly Ash Addition, Considering All Models of Cracking. *IOP Conf. Ser. Mater. Sci. Eng.* **2018**, *416*, 012029. [CrossRef]